IJARSCT

ISSN (Online) 2581-9429

International Journal of Advanced Research in Science, Communication and Technology (IJARSCT)

International Open-Access, Double-Blind, Peer-Reviewed, Refereed, Multidisciplinary Online Journal

Impact Factor: 7.53

Volume 4, Issue 3, April 2024

Unsteady Viscoelastic MHD Fluid Flow through Inclined Porous Plate in the Presence of Heat Source, Thermal Radiation and Chemical Reaction

Nidhi Pandya[1], Priyanka Kannoujia[2] and Pravin Kumar Srivastava[3]

Department of Mathematics and Astronomy, University of Lucknow, Lucknow, Uttar Pradesh, India[1,2]

Bundelkhand Institute of Engineering and Technology, Jhansi, India[3]

dr.nidh23@gmail.com, priyankakannoujia1@gmail.com, drpravinsrivastava@yahoo.com

Abstract*: The unsteady viscoelastic MHD (magnetohydrodynamics) flow via an inclined porous plate embedded in a porous medium showing the radiation and chemical effects are studied in this research. With the use of Mathematica software, dimensionless differential equations of the governing equations of flow are numerically solved using the Crank-Nicolson finite difference method. The discussion of velocity, temperature, and concentration profiles is done using graphs for various parameter values. Skin-friction coefficients, Nusselt number and Sherwood number are discussed through tables for different values of parameters*

Keywords: MHD, Porous media, Soret effect

Nomenclature

- B_0 Strength of magnetic field
- u_0 velocity of plate;
- T Fluid temperature;
- q_r Radioactive heat flux;
- M Magnetic parameter;
- Pr Prandtl number;
- Sr Soret number;
- Gr: Thermal Grashof number;
- Gm: Modified Grashof number;
- k_0: viscoelasticity parameter;
- Γ: non dimensional viscoelastic parameter;
- Q'_0: dimensional heat absorption coeffi cient;
- Q'_1: coefficient of proportionality of the ab- sorption of the radiation;
- Q_0: heat source parameter;
- Q_1: absorption of radiation parameter;
- T_W : wall temperature;
- T_∞: Fluid temperature far away from the plate;
- C_W : Wall concentration;
- C_P : Specific heat at constant pressure;
- C_∞: Concentration far away from the plate;
- u: Dimensionless velocity;
- κ: Thermal conductivity
- g: Gravitational acceleration;
- σ: Electrical conductivity;
- ν: Kinematic viscosity;

- ρ: Fluid density;
- K: Porosity parameter;
- P: Pressure;
- R: Radiation parameter;
- Sc: Schmidt number;
- β_C: Volumetric coefficient of thermal expansion with concentration;
- β_T : Volumetric coefficient of thermal expansion;

I. INTRODUCTION

The study of viscoelastic magnetohydrodynamic (MHD) fluid flow through porous media is a topic of significant interest due to its wide range of applications in engineering and natural sciences. Vis- coelastic fluids, which exhibit both viscous and elastic properties, are often found in industrial pro- cesses involving polymers, biological fluids, and certain lubricants. When these fluids are subjected to a magnetic field, the interactions between the fluid's electrical conductivity and the magnetic forces give rise to complex flow behaviors, which are described by MHD.

Flow through porous media, such as soil, rock, or synthetic materials, is a common phenomenon in various engineering fields, including groundwater hydrology, petroleum engineering, and chemical processing. The porous structure introduces additional resistance to flow, which can significantly alter the fluid dynamics compared to flow in non-porous environments.

It also plays a critical role in biomedical applications, such as drug delivery through porous tissues, and in industrial processes where precise control of fluid flow and heat transfer is necessary. Additionally, understanding the behavior of viscoelastic MHD fluids in porous media is crucial for developing new materials and technologies in environmental engineering, particularly in the remediation of contaminated soils and aquifers.

Theoretical models of viscoelastic MHD fluid flow in porous media often involve complex differ- ential equations that account for the combined effects of fluid elasticity, magnetic fields, and porous resistance. These models help predict the flow behavior under various conditions, enabling engi- neers and scientists to design systems and processes that harness or mitigate these effects. Research in this area continues to evolve, driven by the need for more efficient industrial processes, better environmental management practices, and enhanced understanding of natural fluid systems.

Veera Krishna [1] investigated the unsteady flow of an incompressible visco-elastic liquid described by the Walter B model, focusing on simultaneous heat and mass transfer near an oscillating porous plate in a slip flow regime, while considering the effect of Hall current. Giver and Altobin [2] have discussed the visualization of fluid flow within a porous solid matrix. Kulkarni and Singh [3] examined the unsteady flow between two infinitely long porous parallel plates with a sinusoidally varying pressure gradient, considering a no-slip condition at the solid boundary. Dash and Rath [4] employed an explicit finite difference scheme to analyze the flow and heat transfer of an electrically conducting fluid between porous parallel plates. P.C. Ram [5] investigated The effects of hall and ion slip currents on free convective heat generating flow in a rotating fluid Jitendra and Srinivas [6] investigated the effects of Hall and ion slip on a circulating fluid, while Veera Krishna [7] explored the Hall effect on MHD flow through a porous medium. Veera Krishna [8] examined the Hall effects on the unsteady hydromagnetic natural convective rotating flow of a second-grade fluid past an impulsively moving vertical plate in a saturated porous medium, where the plate's temperature temporarily follows a ramped profile. Veera Krishna [9] studied heat and mass transfer in MHD free convective flow over an infinite, non-conducting vertical flat porous plate. Veera Krishna and Jyothi [10] analyzed the effects of heat and mass transfer on free convective rotating flow of a visco- elastic, incompressible, electrically conducting fluid past a vertical porous plate with time-dependent oscillatory permeability and suction, in the presence of a uniform transverse magnetic field and a heat source. Veera Krishna and Subba Reddy [11] investigated the transient MHD flow of a reactive second-grade fluid through a porous medium between two infinitely long horizontal parallel plates. Mallikarjuna [12] examined the coupled heat and mass transfer in the mixed convection flow of a Newtonian fluid past a rotating vertical cone embedded in a porous medium, considering the effects of a magnetic field and chemical reactions. Veera Krishna [13] explored the Soret and Joule effects in MHD mixed convective flow of an incompressible, electrically conducting viscous fluid past an infinite vertical porous plate, incorporating the Hall

IJARSCT

ISSN (Online) 2581-9429

International Journal of Advanced Research in Science, Communication and Technology (IJARSCT)

International Open-Access, Double-Blind, Peer-Reviewed, Refereed, Multidisciplinary Online Journal

Impact Factor: 7.53

Volume 4, Issue 3, April 2024

effects. M. G. Reddy [14] studied thermal radiation and chemical reaction effects on steady convective slip flow with uniform heat and mass flux in the presence of ohmic heating and a heat source.

The main objective is to investigate the unsteady viscoelastic MHD fluid flow through an inclined porous plate in the presence of a heat source, thermal radiation, and chemical reactions.The implicit finite difference approach of Crank-Nicolson is used to solve numerically the governing equation of the non-dimensional form of flow fields. Graphs are used to illustrate the effects of various physical parameters on temperature, concentration, and velocity.

II. FORMULATION

Consider an unsteady MHD flow of a viscoelastic incompressible electrically conducting fluid past an infinite inclined porous plate is analyzed. Plate is embedded in porous medium and inclined at angle λ to the vertical. x'-axis is taken along the plate and y'-axis is normal to it. A variable magnetic field B_0 is taken in perpendicular to flow field and plate is electrically non-conducting. Consider y'-axis normal to x'-z' plane.

Initially the plate and fluid are at the same temperature and concentration $T_\infty{}'$ and $C_\infty{}'$ re- spectively. At time $t' > 0$ plate is given in motion along x'- direction with constant velocity u_0. A transverse magnetic field B_0 is considered normal to the direction of flow. Magnetic Reynold number and transversely applied magnetic field are very small, therefore induced magnetic field is negligible. Due to infinite length in x'- direction the flow variables are functions of y' and t' only. Under the above assumptions,the governing boundary layer equations with Boussinesq's approximation are: Momentum equation:

$$\frac{\partial u'}{\partial t'} = \nu \frac{\partial^2 u'}{\partial y'^2} + g\beta_T (T' - T_\infty{}')cos\lambda + g\beta_C (C' - C_\infty{}')cos\lambda - k_0 \frac{\partial^3 u'}{\partial y'^2 \partial t'} - (\frac{\sigma B_0{}^2}{\rho})u' - \frac{\nu}{K'}u' \quad (2.1)$$

Energy equation:

$$\frac{\partial T'}{\partial t'} = \frac{\kappa}{\rho C_P}\frac{\partial^2 T'}{\partial y'^2} - \frac{\partial q_r}{\partial y'} - \frac{Q_0'}{\rho C_P}(T' - T_\infty{}') + Q_1'(C' - C_\infty{}') \quad (2.2)$$

Mass transfer equation:

$$\frac{\partial C'}{\partial t'} = D\frac{\partial^2 C'}{\partial y'^2} - K_r'(C' - C_\infty{}') \quad (2.3)$$

The boundary conditions are:

$$t' \leq 0; u' = 0, T' = T_\infty{}', C' = C_\infty{}' \quad \forall y'$$

$$t' > 0, u' = u_0 t, T' = T_W{}', C' = C_W{}' \quad at \quad y' = 0$$

$$u' \to 0, T' \to T_\infty{}', C' \to C_\infty{}' \quad as \quad y' \to \infty \quad (2.4)$$

Radiative heat flux term using the Roselnd approximation is given by

$$q_r = -\frac{4\sigma'}{3k_m}\frac{\partial T'^4}{\partial y'} \quad (2.5)$$

In this equation, σ denotes the Stefan–Boltzmann Constant, while k1 is the mean absorption coeffi- cient. By extending T ∗4 in a Taylor series around T∞∗, and ignoring higher order components, we may get a linear version if the temperature gradients within the flow are small sufficiently in the form

$$T'^4 \cong 4T'_\infty{}^3 T' - 3T'_\infty{}^3 \quad (2.6)$$

Using equations (2.5) and (2.6), equation (2.2) becomes

IJARSCT
ISSN (Online) 2581-9429
International Journal of Advanced Research in Science, Communication and Technology (IJARSCT)
International Open-Access, Double-Blind, Peer-Reviewed, Refereed, Multidisciplinary Online Journal
Impact Factor: 7.53
Volume 4, Issue 3, April 2024

$$\frac{\partial T'}{\partial t'} = \frac{\kappa}{\rho C_P}\frac{\partial^2 T'}{\partial y'^2} + \frac{16\sigma' T'_\infty{}^3}{3k_m}\frac{\partial^2 T'}{\partial y'^2} - \frac{Q'_0}{\rho C_P}(T' - T_\infty') + Q'_1(C' - C_\infty') \tag{2.7}$$

The following non dimensional quantities are introduced:

$$u = \frac{u'}{u_0}, t = \frac{t' u_0{}^2}{\nu}, y = \frac{u_0 y'}{\mu}, \theta = \frac{(T' - T'_\infty)}{(T'_W - T'_\infty)}, \phi = \frac{(C' - C'_\infty)}{(C'_W - C'_\infty)}, Gr = \frac{\nu g \beta_T (T_w' - T_\infty')}{u_0'^3},$$

$$Gm = \frac{\nu g \beta_C (C_w' - C_\infty')}{u_0'^3}, K = \frac{u_0{}^2 K'}{\nu^2}, M = \frac{\sigma B_0{}^2 \nu}{\rho u_0{}^2}, Pr = \frac{\mu C_P}{k'}, \Gamma = \frac{k_0 u_0{}^2}{\nu^2}, R = \frac{4\sigma T_\infty'^3}{k_1 k},$$

$$Q_0 = \frac{Q'_0 \nu}{\rho C_p u_0{}^2}, Q_1 = \frac{Q'_1 \nu (C_w - C_\infty)}{u_0{}^2 (T_w - T_\infty)} Sc = \frac{\nu}{D_M}$$

It is possible to simplify equations using dimensionless values.

$$\frac{\partial u}{\partial t} = \frac{\partial^2 u}{\partial y^2} + Grcos\lambda\theta + Gm\phi cos\lambda\theta - \Gamma\frac{\partial^3 u}{\partial y^2 \partial t} - (M + \frac{1}{K})u \tag{2.8}$$

$$\frac{\partial \theta}{\partial t} = \frac{1}{Pr}\left(1 + \frac{4R}{3}\right)\frac{\partial^2 \theta}{\partial y^2} - Q_0\theta + Q_1\phi \tag{2.9}$$

$$\frac{\partial \phi}{\partial t} = \frac{1}{Sc}\frac{\partial^2 \phi}{\partial y^2} - K_r\phi \tag{2.10}$$

The appropriate non-dimensional boundary conditions are

$t \le 0;\ u = 0,\ \theta = 0,\ \phi = 0\ \forall y$

$t > 0,\ u = t,\ \theta = 1,\ \phi = 1$ at $y = 0$

$u \to 0,\ \theta \to 0,\ \phi \to 0$ as $y \to \infty$ (2.11)

Currently, many researchers are interested in calculating physical quantities such as the skin- friction coefficient along the x-axis, the Nusselt number (Nu), and the Sherwood number (Sh). The non-dimensional forms of these quantities are as follows:

Skin friction is given by:

$$\tau = \left(\frac{\partial u}{\partial y}\right)_{y=0} \tag{2.12}$$

Nusselt number is given by:

$$Nu = -\left(\frac{\partial \theta}{\partial y}\right)_{y=0} \tag{2.13}$$

Sherwood number is given by:

$$Sh = -\left(\frac{\partial \phi}{\partial y}\right)_{y=0} \tag{2.14}$$

III. SOLUTION OF THE PROBLEM

After setting up the proper initial and boundary conditions, the non-linear momentum, and energy equations, and may be resolved by employing the implicit finite difference approach of the Crank and Nicolson model that is being employed. Using the Nicolson approach, we discretize the appropriate finite difference equations

IJARSCT

ISSN (Online) 2581-9429

International Journal of Advanced Research in Science, Communication and Technology (IJARSCT)

International Open-Access, Double-Blind, Peer-Reviewed, Refereed, Multidisciplinary Online Journal

Impact Factor: 7.53

Volume 4, Issue 3, April 2024

$$\frac{u_{i,j+1}-u_{i,j}}{\Delta t} = (\frac{u_{i-1,j}-2u_{i,j}+u_{i+1,j}+u_{i-1,j+1}-2u_{i,j+1}+u_{i+1,j+1}}{2(\Delta y)^2}) + Grcos(\lambda)(\frac{\theta_{i,j+1}+\theta_{i,j}}{2})$$
$$+Gmcos(\lambda)(\frac{\phi_{i,j+1}+\phi_{i,j}}{2}) - (\frac{u_{i-1,j}-2u_{i,j}+u_{i+1,j}+u_{i-1,j+1}-2u_{i,j+1}+u_{i+1,j+1}}{2(\Delta y)^2\Delta t})$$
$$-(M+\frac{1}{K})(\frac{u_{i,j+1}+u_{i,j}}{2}) \quad (3.1)$$

$$\frac{\theta_{i,j+1}-\theta_{i,j}}{\Delta t} = \frac{1}{Pr}(\frac{\theta_{i-1,j}-2\theta_{i,j}+\theta_{i+1,j}+\theta_{i-1,j+1}-2\theta_{i,j+1}+\theta_{i+1,j+1}}{2(\Delta y)^2}) - Q_0(\frac{\theta_{i,j+1}+\theta_{i,j}}{2})$$
$$+Q_1(\frac{\phi_{i,j+1}+\phi_{i,j}}{2}) \quad (3.2)$$

$$\frac{\phi_{i,j+1}-\phi_{i,j}}{\Delta t} = \frac{1}{Sc}(\frac{\phi_{i-1,j}-2\phi_{i,j}+\phi_{i+1,j}+\phi_{i-1,j+1}-2\phi_{i,j+1}+\phi_{i+1,j+1}}{2(\Delta y)^2})$$
$$+Sr(\frac{\theta_{i-1,j}-2\theta_{i,j}+\theta_{i+1,j}+\theta_{i-1,j+1}-2\theta_{i,j+1}+\theta_{i+1,j+1}}{2(\Delta y)^2}) \quad (3.3)$$

corresponding boundary conditions

$$u_{i,0}=0, \theta_{i,0}=0, \phi_{i,0}=0 \quad \forall i$$

$$u_{0,j}=t, \theta_{0,j}=1, \phi_{0,j}=1 \quad \forall j$$

$$u_{L,j}\to 0, \theta_{L,j}\to 0, \phi_{L,j}\to 0 \quad (3.4)$$

Here, the index i refers to y, and j represents time. Additionally, Δt = tj+1 tj and Δy = yi+1 yi. Given the values of u, θ, and ϕ at time t, the values at t + Δt can be calculated as follows, By substituting i=1,2,3,. . . ,L1 into the equations, which form a tridiagonal system, we can solve using the Thomas algorithm. This provides the values of θ and ϕ for all y at t +Δt. These values are then substituted into the equation and solved using the same procedure, with the initial and boundary conditions, to obtain the solution for u upto the desired time t.

IV. RESULTS AND DISCUSSION

The velocity, concentration, and temperature profiles are presented through graphs for various values of flow parameters. The impact of several parameters, including the porosity parameter K, solutal Grashof number Gm, magnetic parameter M, thermal Grashof number Gr, and radiation parameter R, on velocity distribution, temperature, and concentration fields has been analyzed and illustrated graphically, as shown in Figures 1-16. In this work, the following default values of different parame- ters are used for computations: Gr = 3; Gm = 3; K = 0.9; M = 3; Pr = 0.71; Sc = 0.66; Kr = 2; t = 1; Q0 = 1; Q1 = 1; R = 2; Γ = 0.0005; α = 30o.

Figures 1 and 2 demonstrate that increasing the thermal Grashof number and solutal Grashof number leads to a rise in velocity. In Figures 3 and 4, velocity decreases as the viscoelasticity parameter and magnetic parameter increase, respectively. As shown in Figure 5, an increase in the porosity parameter results in higher velocity. Furthermore, Figures 6-8 reveal that the velocity decreases with increasing Prandtl number, Schmidt number, and inclined angle, respectively. Figures 9 and 10 illustrate that velocity increases with higher radiation parameter and time. Figures 11 and 12 show the effects of Prandtl number and heat source parameter on temperature, with temperature decreasing as both parameters increase. In Figures 13 and 14, temperature rises with an increase in the absorption of radiation parameter and radiation parameter. Figure 15 highlights the effect of Schmidt number on concentration, showing that concentration decreases as the Schmidt number increases. Lastly, Figure 16 demonstrates that increasing the chemical reaction parameter leads to a decrease in fluid concentration.

IJARSCT
ISSN (Online) 2581-9429
International Journal of Advanced Research in Science, Communication and Technology (IJARSCT)
International Open-Access, Double-Blind, Peer-Reviewed, Refereed, Multidisciplinary Online Journal
Impact Factor: 7.53
Volume 4, Issue 3, April 2024

Table 1 shows the comparison of present study with M. G. Reddy [14] for different values of different parameters where the present work is an unsteady problem as compared to the work of M. G. Reddy [14] which was steady problem and boundary conditions are also different. The skin friction, nusselt number and sherwood number are presented in Table [2-3], Table 5 and Table 4 respectively, where the effect of various parameters on skin friction, nusselt number and sherwood number is displayed.

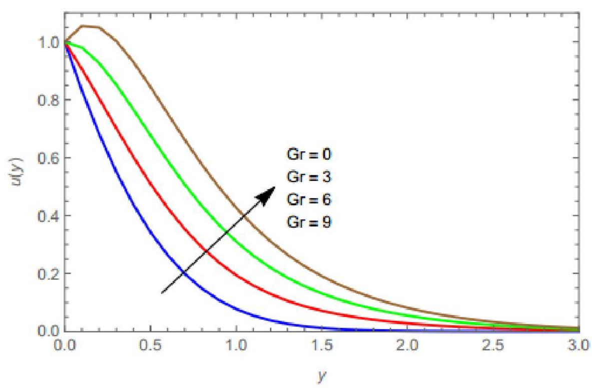

Figure 1: Variation of Thermal Grashof number on velocity

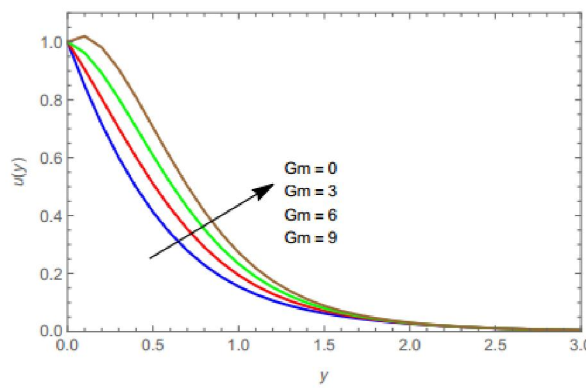

Figure 2: Variation of Solutal Grashof number on velocity

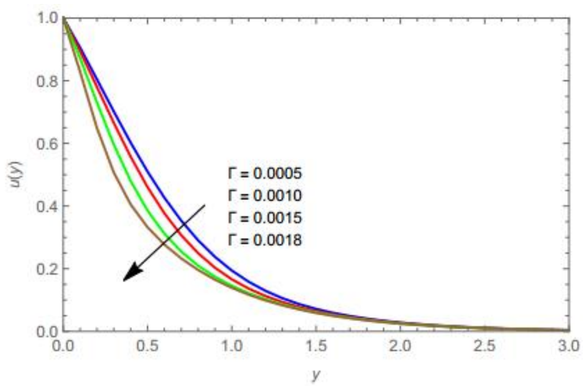

Figure 3: Variation of viscoelasticity parameter on velocity

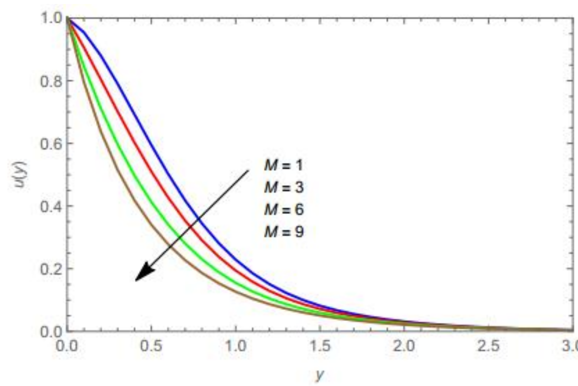

Figure 4: Variation of Magnetic parameter on velocity

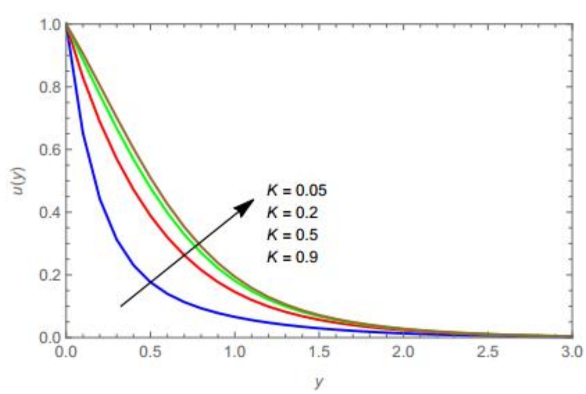

Figure 5: Variation of porosity parameter on velocity

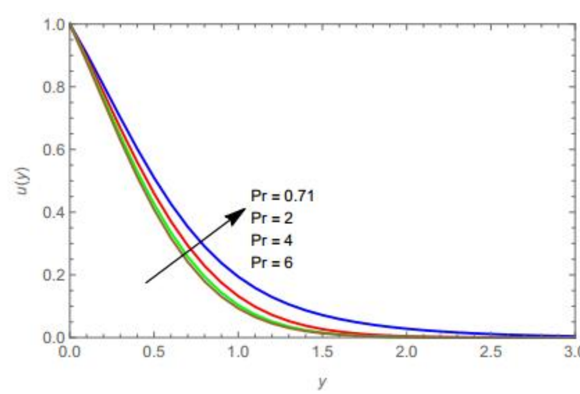

Figure 6: Variation of Prandtl number on velocity

DOI: 10.48175/568
ISSN 2581-9429 IJARSCT

IJARSCT
ISSN (Online) 2581-9429
International Journal of Advanced Research in Science, Communication and Technology (IJARSCT)
International Open-Access, Double-Blind, Peer-Reviewed, Refereed, Multidisciplinary Online Journal
Impact Factor: 7.53
Volume 4, Issue 3, April 2024

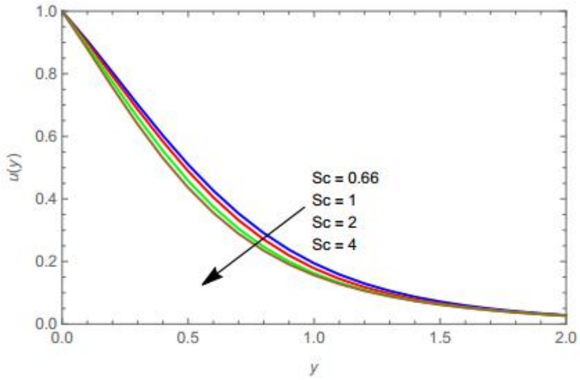

Figure 7: Variation of Schmidt number on velocity

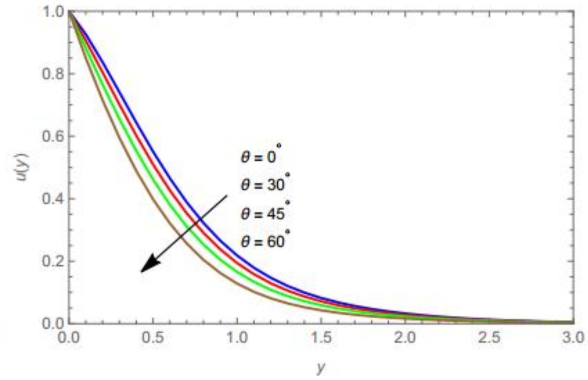

Figure 8: Variation of angle on velocity

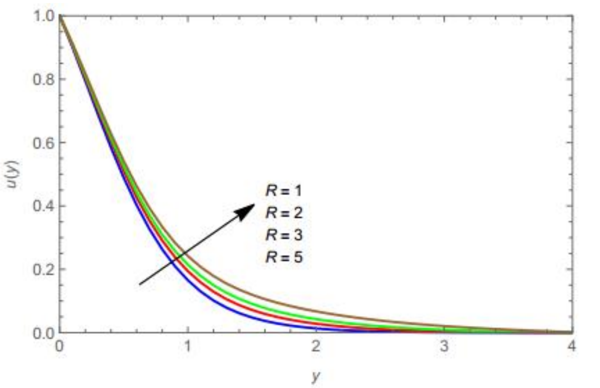

Figure 9: Variation of radiation parameter on velocity

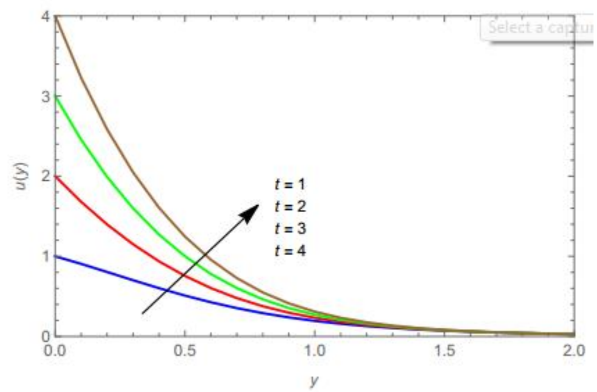

Figure 10: Variation of time on velocity

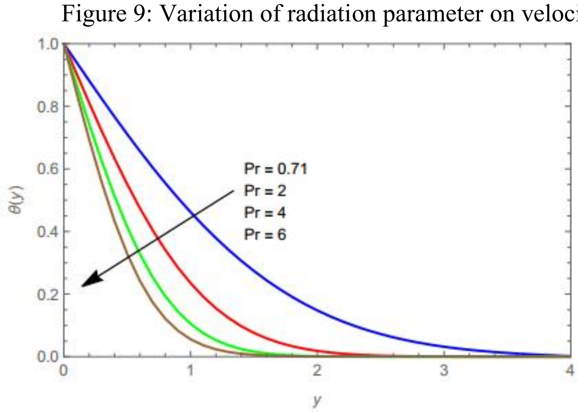

Figure 11: Variation of Prandtl number on temperature

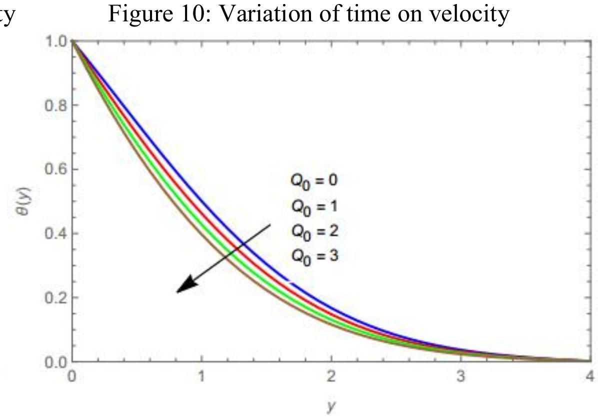

Figure 12: Variation of heat source parameter on temperature

V. CONCLUSION

In this work, we have unsteady viscoelastic MHD fluid flow through inclined porous plate in the presence of heat source, thermal radiation and chemical reaction which have following conclusions:

DOI: 10.48175/568

IJARSCT
ISSN (Online) 2581-9429
International Journal of Advanced Research in Science, Communication and Technology (IJARSCT)
International Open-Access, Double-Blind, Peer-Reviewed, Refereed, Multidisciplinary Online Journal
Impact Factor: 7.53
Volume 4, Issue 3, April 2024

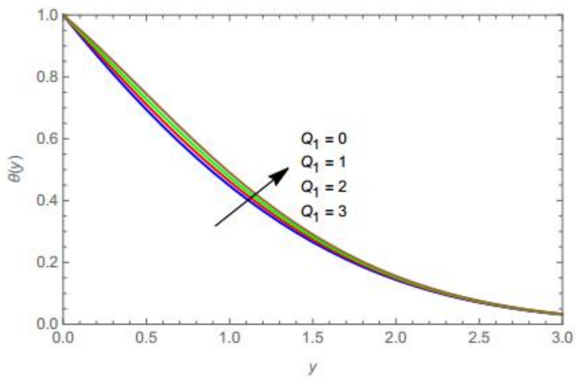

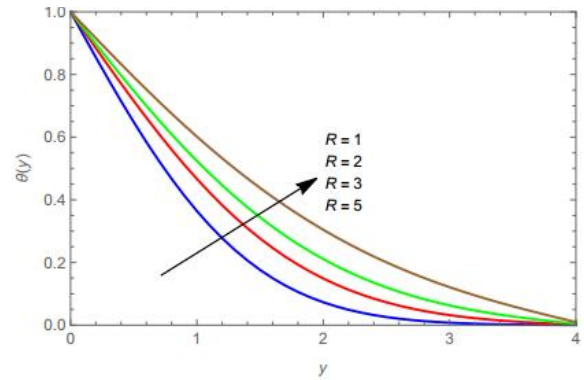

Figure 13: Variation of absorption of radiation parameter on temperature

Figure 14: Variation of radiation parameter on temperature

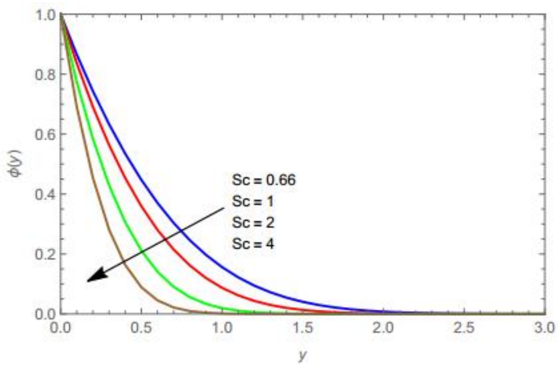

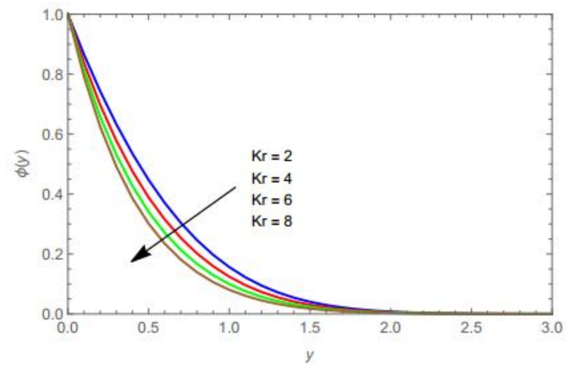

Figure 15: Variation of Schmidt number on con- centration

Figure 16: Variation of chemical reaction pa- rameter on concentration

Table 1: Comparison of present results with those of M. G. Reddy [14] with different values with different parameters on skin friction

Different physical parameters	**τ (M. G. Reddy)**	**τ (present result)**
$Gr = 2,\ Gm = 2,\ M = 2,\ K = 0.5$	0.8064	-1.34136
$Gr = 4,\ Gm = 2,\ M = 2,\ K = 0.5$	1.1517	-0.834934
$Gr = 2,\ Gm = 4,\ M = 2,\ K = 0.5$	1.2697	-0.951957
$Gr = 2,\ Gm = 2,\ M = 4,\ K = 0.5$	0.4137	-1.72867
$Gr = 2,\ Gm = 2,\ M = 2,\ K = 1.0$	0.8907	-1.12593

Table 2: Skin friction for different values of parameter

Gr	**Gm**	**K**	**M**	**Pr**	**Sc**	**Kr**	**t**	Q_0	Q_1	**R**	Γ	λ	τ
0	3	0.9	3	0.71	0.66	2	1	1	1	2	0.0005	30^0	-1.68741
3	3	0.9	3	0.71	0.66	2	1	1	1	2	0.0005	30^0	-0.94209
6	3	0.9	3	0.71	0.66	2	1	1	1	2	0.0005	30^0	-0.19677
9	3	0.9	3	0.71	0.66	2	1	1	1	2	0.0005	30^0	0.54855
3	**0**	0.9	3	0.71	0.66	2	1	1	1	2	0.0005	30^0	-1.51051
3	**3**	0.9	3	0.71	0.66	2	1	1	1	2	0.0005	30^0	-0.94209
3	**6**	0.9	3	0.71	0.66	2	1	1	1	2	0.0005	30^0	-0.373668
3	**9**	0.9	3	0.71	0.66	2	1	1	1	2	0.0005	30^0	0.194754
3	3	0.9	3	0.71	0.66	2	1	1	1	2	**0.0005**	30^0	-0.94209
3	3	0.9	3	0.71	0.66	2	1	1	1	2	**0.0010**	30^0	-1.05141

3	3	0.9	3	0.71	0.66	2	1	1	1	2	**0.0015**	30^0	-1.28037
3	3	0.9	3	0.71	0.66	2	1	1	1	2	**0.0018**	30^0	-1.71609
3	3	0.9	**1**	0.71	0.66	2	1	1	1	2	0.0005	30^0	-0.458849
3	3	0.9	**3**	0.71	0.66	2	1	1	1	2	0.0005	30^0	-0.94209
3	3	0.9	**6**	0.71	0.66	2	1	1	1	2	0.0005	30^0	-1.54782
3	3	0.9	**9**	0.71	0.66	2	1	1	1	2	0.0005	30^0	-2.04571
3	3	**0.05**	3	0.71	0.66	2	1	1	1	2	0.0005	30^0	-3.48056
3	3	**0.2**	3	0.71	0.66	2	1	1	1	2	0.0005	30^0	-1.70512
3	3	**0.5**	3	0.71	0.66	2	1	1	1	2	0.0005	30^0	-1.13492
3	3	**0.9**	3	0.71	0.66	2	1	1	1	2	0.0005	30^0	-0.94209
3	3	0.9	3	**0.71**	0.66	2	1	1	1	2	0.0005	30^0	-0.94209
3	3	0.9	3	**2**	0.66	2	1	1	1	2	0.0005	30^0	-1.05968
3	3	0.9	3	**4**	0.66	2	1	1	1	2	0.0005	30^0	-1.14873
3	3	0.9	3	**6**	0.66	2	1	1	1	2	0.0005	30^0	-1.20254
3	3	0.9	3	0.71	0.66	2	1	**0**	1	2	0.0005	30^0	-0.926534
3	3	0.9	3	0.71	0.66	2	1	**1**	1	2	0.0005	30^0	-0.94209
3	3	0.9	3	0.71	0.66	2	1	**2**	1	2	0.0005	30^0	-0.956707
3	3	0.9	3	0.71	0.66	2	1	**3**	1	2	0.0005	30^0	-0.97047

Table 3: Skin friction for different values of parameter

Gr	Gm	K	M	Pr	Sc	Kr	t	Q_0	Q_1	R	Γ	λ	τ
3	3	0.9	3	0.71	0.66	2	1	1	**0**	2	0.0005	30^0	-0.950288
3	3	0.9	3	0.71	0.66	2	1	1	**1**	2	0.0005	30^0	-0.94209
3	3	0.9	3	0.71	0.66	2	1	1	**2**	2	0.0005	30^0	-0.933892
3	3	0.9	3	0.71	0.66	2	1	1	**3**	2	0.0005	30^0	-0.925694
3	3	0.9	3	0.71	**0.66**	2	1	1	1	2	0.0005	30^0	-0.94209
3	3	0.9	3	0.71	**1**	2	1	1	1	2	0.0005	30^0	-1.00231
3	3	0.9	3	0.71	**2**	2	1	1	1	2	0.0005	30^0	-1.10453
3	3	0.9	3	0.71	**4**	2	1	1	1	2	0.0005	30^0	-1.2034
3	3	0.9	3	0.71	0.66	**2**	1	1	1	2	0.0005	30^0	-0.94209
3	3	0.9	3	0.71	0.66	**4**	1	1	1	2	0.0005	30^0	-0.974605
3	3	0.9	3	0.71	0.66	**6**	1	1	1	2	0.0005	30^0	-1.00304
3	3	0.9	3	0.71	0.66	**8**	1	1	1	2	0.0005	30^0	-1.02809
3	3	0.9	3	0.71	0.66	2	1	1	1	2	0.0005	0^0	-0.738853
3	3	0.9	3	0.71	0.66	2	1	1	1	2	0.0005	30^0	-0.94209
3	3	0.9	3	0.71	0.66	2	1	1	1	2	0.0005	45^0	-1.18317
3	3	0.9	3	0.71	0.66	2	1	1	1	2	0.0005	60^0	-1.49734
3	3	0.9	3	0.71	0.66	2	1	1	1	**1**	0.0005	30^0	-0.990555
3	3	0.9	3	0.71	0.66	2	1	1	1	**2**	0.0005	30^0	-0.94209
3	3	0.9	3	0.71	0.66	2	1	1	1	**3**	0.0005	30^0	-0.911716
3	3	0.9	3	0.71	0.66	2	1	1	1	**5**	0.0005	30^0	-0.873877
3	3	0.9	3	0.71	0.66	2	**1**	1	1	2	0.0005	30^0	-0.94209
3	3	0.9	3	0.71	0.66	2	**2**	1	1	2	0.0005	30^0	-3.19792
3	3	0.9	3	0.71	0.66	2	**3**	1	1	2	0.0005	30^0	-5.45375
3	3	0.9	3	0.71	0.66	2	**4**	1	1	2	0.0005	30^0	-7.70958

IJARSCT
ISSN (Online) 2581-9429
International Journal of Advanced Research in Science, Communication and Technology (IJARSCT)
International Open-Access, Double-Blind, Peer-Reviewed, Refereed, Multidisciplinary Online Journal
Impact Factor: 7.53
Volume 4, Issue 3, April 2024

Table 4: Sherwood number for different values of parameter

Gr	Gm	K	M	Pr	Sc	Kr	t	Q_0	Q_1	R	Γ	λ	Sh
3	3	0.9	3	0.71	**0.66**	2	1	1	1	2	0.0005	30^0	1.34618
3	3	0.9	3	0.71	**1**	2	1	1	1	2	0.0005	30^0	1.63884
3	3	0.9	3	0.71	**2**	2	1	1	1	2	0.0005	30^0	2.26139
3	3	0.9	3	0.71	**4**	2	1	1	1	2	0.0005	30^0	3.08726
3	3	0.9	3	0.71	0.66	**2**	1	1	1	2	0.0005	30^0	1.34618
3	3	0.9	3	0.71	0.66	**4**	1	1	1	2	0.0005	30^0	1.62473
3	3	0.9	3	0.71	0.66	**6**	1	1	1	2	0.0005	30^0	1.8695
3	3	0.9	3	0.71	0.66	**8**	1	1	1	2	0.0005	30^0	2.08699

Table 5: Nusselt number for different values of parameter

Gr	Gm	K	M	Pr	Sc	Kr	t	Q_0	Q_1	R	Γ	λ	Nu
3	3	0.9	3	**0.71**	0.66	2	1	1	1	2	0.0005	30^0	0.593132
3	3	0.9	3	**2**	0.66	2	1	1	1	2	0.0005	30^0	0.951463
3	3	0.9	3	**4**	0.66	2	1	1	1	2	0.0005	30^0	1.30095
3	3	0.9	3	**6**	0.66	2	1	1	1	2	0.0005	30^0	1.56099
3	3	0.9	3	0.71	0.66	2	1	**0**	1	2	0.0005	30^0	0.493802
3	3	0.9	3	0.71	0.66	2	1	**1**	1	2	0.0005	30^0	0.593132
3	3	0.9	3	0.71	0.66	2	1	**2**	1	2	0.0005	30^0	0.685861
3	3	0.9	3	0.71	0.66	2	1	**3**	1	2	0.0005	30^0	0.772707
3	3	0.9	3	0.71	0.66	2	1	1	**0**	2	0.0005	30^0	0.65395
3	3	0.9	3	0.71	0.66	2	1	1	**1**	2	0.0005	30^0	0.593132
3	3	0.9	3	0.71	0.66	2	1	1	**2**	2	0.0005	30^0	0.532314
3	3	0.9	3	0.71	0.66	2	1	1	**3**	2	0.0005	30^0	0.471496
3	3	0.9	3	0.71	**0.66**	2	1	1	1	2	0.0005	30^0	0.593132
3	3	0.9	3	0.71	**1**	2	1	1	1	2	0.0005	30^0	0.602364
3	3	0.9	3	0.71	**2**	2	1	1	1	2	0.0005	30^0	0.615979
3	3	0.9	3	0.71	**4**	2	1	1	1	2	0.0005	30^0	0.627155
3	3	0.9	3	0.71	0.66	**2**	1	1	1	2	0.0005	30^0	0.593132
3	3	0.9	3	0.71	0.66	**4**	1	1	1	2	0.0005	30^0	0.598067
3	3	0.9	3	0.71	0.66	**6**	1	1	1	2	0.0005	30^0	0.602246
3	3	0.9	3	0.71	0.66	**8**	1	1	1	2	0.0005	30^0	0.605815
3	3	0.9	3	0.71	0.66	2	1	1	1	**1**	0.0005	30^0	0.729684
3	3	0.9	3	0.71	0.66	2	1	1	1	**2**	0.0005	30^0	0.593132
3	3	0.9	3	0.71	0.66	2	1	1	1	**3**	0.0005	30^0	0.514023
3	3	0.9	3	0.71	0.66	2	1	1	1	**5**	0.0005	30^0	0.421651

- On increasing viscoelasticity parameter, magnetic parameter, Prandtl number, Schmidt num- ber and inclined angle, velocity decreases.
- Velocity increases on increasing thermal and solutal Grashof number, porosity, radiation pa- rameter and time.
- Temperature falls on increasing Prandtl number and heat source parameter.
- Temperature increases on increasing absorption of radiation parameter, radiation parameter
- Concentration decreases on increasing Schmidt number and chemical reaction parameter.

REFERENCES

[1]. M.V. Krishna, Hall effects on MHD flow of a visco-elastic fluid through a porous medium over an infinite oscillating porous plate with heat source and chemical reaction, Interna- tional Journal of Computer Aided Engineering & Technology, **11** (6), (2019), 679–698, https://doi.org/10.1504/IJCAET.2019.102498

[2]. R.C. Givler, S.A. Altobelli, A determination of the effective viscosity for the Brinkman- Forch- heimer flow model, J. Fluid Mech., 258, (1994), 355.

[3]. S.B. Kulkarni, B.B. Singh, Unsteady laminar flow of elastico-viscous fluid between two parallel plates, Ind, J. Eng. Mater. Sci., **12** (2005) 51–57.

[4]. G.C. Dash, P.K. Rath, Explicit finite difference scheme for flow and heat transfer of an elec- trically conducting fluid between porous parallel plates, Proc. Nat. Acad. Sci. India, **67** (A), (1997) II.

[5]. P.C. Ram, The effects of hall and ion slip currents on free convective heat generating flow in a rotating fluid, Int. J. Energy Res.,**19** (5), (1995), 371–376, https://doi.org/ 10.1002/er.4440190502.

[6]. J.K. Singh, S. C.T, Unsteady natural convection flow of a rotating fluid past an exponential accelerated vertical plate with Hall current, ion-slip and magnetic effect, Multidiscip. Model. Mater. Struct., **14** (2), (2018), 216–235, https://doi.org/10. 1108/MMMS-06-2017-0045.

[7]. M. V. Krishna, G. Subba Reddy, A.J. Chamkha, Hall effects on unsteady MHD oscillatory free convective flow of second-grade fluid through the porous medium between two vertical plates, Phys. Fluids, **30**, (2018), 023106, , https://doi.org/10. 1063/1.5010863.

[8]. M. V. Krishna, M. G. Reddy, A.J. Chamkha, Heat and mass transfer on MHD rotating flow of second grade fluid past an infinite vertical plate embedded in uniform porous medium with Hall effects, Applied Mathematics and Scientific Computing, Trends in Mathematics, **1**, (2019), 417–427, https://doi.org/10.1007/978-3-030-01123-9_41.

[9]. M. V. Krishna, M. G. Reddy, A.J. Chamkha, Heat and mass transfer on MHD free convective flow over an infinite non-conducting vertical flat porous plate, Int. Jour. of Fluid Mech. Res., **45** (5), (2019), 1–25, https://doi.org/10.1615/ InterJFluidMechRes.2018025004.

[10]. M. V. Krishna, K. Jyothi, Heat and mass transfer on MHD rotating flow of a visco-elastic fluid through porous medium with time dependent oscillatory permeability, J. Therm. Anal., **27** (2), (2018), 1–19, https://doi.org/10.1007/s41478-018-0099-0.

[11]. M. V. Krishna, G. S. Reddy, Unsteady MHD reactive flow of second grade fluid through porous medium in a rotating parallel plate channel, J. Therm. Anal., **27** (1), (2019), 103–120, https://doi.org/10.1007/s41478-018-0108-3.

[12]. B. Mallikarjuna, A.M. Rashad, A.J. Chamkha, S.H. Raju, Chemical reaction effects on MHD convective heat and mass transfer flow past a rotating vertical cone embedded in a variable porosity regime, Afrika Matematica, **27**, (2016), 645–665, https://doi.org/10.1007/s13370-015- 0372-1.

[13]. M. V. Krishna, B.V. Swarnalathamma, A.J. Chamkha, Investigations of Soret, Joule and Hall effects on MHD rotating mixed convective flow past an infinite vertical porous plate, Journal of Ocean Engineering and Science, **4** (3), (2019), 263–275, https://doi.org/10.1016/j.joes.2019.05.002 .

[14]. M. G. Reddy, Thermal radiation and chemical reaction effects on steady convective slip flow with uniform heat and mass flux in the presence of ohmic heating and a heat source, FDMP, **10**, (4),2014, 417-442, DOI: 10.3970/fdmp.2014.010.417